Microfluidics and Nanofluidics (2023) 27:11
https://doi.org/10.1007/s10404-022-02619-y

RESEARCH PAPER

Development of microfluidic platform that enables 'on-chip' imaging of cells exposed to shear stress and cyclic stretch

Whitney E. Sinclair[1] · Ashtamurthy S. Pawate[1] · Ty'Nya A. Larry[1] · Jeremy M. Schieferstein[1] · Joseph J. Whittenberg[1] · Deborah E. Leckband[1,2,3] · Paul J. A. Kenis[1,3]

Received: 29 August 2022 / Accepted: 19 December 2022 / Published online: 10 January 2023

Abstract

Here, we describe the development of an organ-on-a-chip platform that enables ex vivo studies under active physio-mechanical stress by applying hydrodynamic and mechanical forces to vascular endothelial cells. Access to current platforms for such studies is hampered by the need for advanced fabrication techniques to create these platforms, and the need for extensive ancillary equipment for their operation. The platform design and fabrication approach reported here aims to improve accessibility of microfluidic technology for ex vivo mechanobiology studies to the broader biomedical research community. Dual-layer lithography was used to significantly reduce the technical expertise and equipment required to create porous, stretchable membranes that serve as the substrate for cells. A cost-effective, portable pressure regulator was created to apply physiologically relevant cyclic stretch (to resemble breathing) across pulmonary endothelial cells grown on the porous membrane. The use of cyclic olefin copolymer sheets helped reduce the total thickness of the microfluidic platform to about 3 mm, enabling fluorescence imaging 'on-chip'. Furthermore, the reversible bond between the cyclic olefin copolymer lid and the rest of the platform allows for exposure of the cells to aerosolized particulates. To validate the capacity to image cells in situ, we obtained subcellular actin images of bovine aortic endothelial cells and human pulmonary aortic endothelial cells 'on-chip'. Overall, we present an accessible microfluidic platform that exposes endothelial cells to physiologically relevant shear and/or cyclic stretch, and allows for post exposure 'on-chip' cell imaging.

Keywords Confocal imaging 'on-chip' · Pressure regulator · Microfluidics · Lung-on-a-chip development

1 Introduction

'Organ-on-chip' platforms aim to recapitulate complex tissue physiology in vitro (Huh et al. 2010; Bhatia and Ingber 2014; Beißner et al. 2016; Pattanayak et al. 2021). In principle, 'organ-on-chip' devices can be engineered to generate similar mechanical and hydrodynamic forces experienced by cells in vivo (Huh et al. 2012a, 2012b; Dudek and Garcia 2001). For example, lung-on-a-chip models mimic functional pulmonary lung tissue and have the ability to apply coordinated shear stress and/or cyclic stretch. With the ability to apply coordinated shear stress and cyclic stretch, lung-on-a-chip platforms can be translated to recapitulate endothelial function.

A range of mechanical and hydrodynamic cues influence vascular endothelial function (Hahn and Schwartz 2009). During inhalation and exhalation at the alveoli, the surrounding pulmonary endothelium undergo stretching and relaxation (cyclic stretch). In vivo lung alveoli experience physiological levels of mechanical strain corresponding to 5–12% linear distension (Tschumperlin et al. 2000; Birukov et al. 2003; Dan et al. 2016). Hydrodynamic forces, acting on the endothelial cells, are a result of blood flowing throughout the body (shear stress). Fluid shear stress in physiological conditions spans from 1 to 70 dynes/cm^2, depending on the type of blood vessel (Tzima et al. 2005; Charbonier et al. 2019; Malek et al. 1999).

✉ Paul J. A. Kenis
kenis@illinois.edu

[1] Department of Chemical and Biomolecular Engineering, University of Illinois at Urbana-Champaign, Urbana, IL 61801, USA

[2] Department of Chemistry, University of Illinois at Urbana-Champaign, Urbana, IL 61801, USA

[3] Carl Woese Institute for Genomic Biology, University of Illinois at Urbana-Champaign, Urbana, IL 61801, USA

Ingber et al. pioneered the development of microfluidic lung-on-a-chip platforms (Huh et al. 2010; Benam et al. 2016a, 2016b; Jain et al. 2018). While other laboratories have created their own lung-on-a-chip platforms (Humayun et al. 2018; Zhang et al. 2021; Meghani et al. 2020; Yang et al. 2018), platforms with shear stress and cyclic stretch capabilities are limited to platforms established in the Ingber et al. and Guenat et al. (Stucki et al. 2015) laboratories. In a review of in vitro pulmonary platform, Artzy-Schnirman et al. states that "*the need for rather complex actuation systems (e.g., vacuum pressure pumps) in conjunction with advanced microfabrication techniques… are still hampering a wider spread use of such setups across the respiratory research community* (Artzy-Schnirman et al. 2021)."

Here, we report the fabrication of a microfluidic platform that facilitates the exposure of cells to physiologically relevant shear stress and cyclic stretch while allowing for imaging 'on-chip' of these cells. Our platform design aims to improve platform accessibility to the biomedical community by reducing technical expertise and equipment required for platform fabrication and application. Specially, by utilizing a dual-layer lithography technique, we obtained a fully integrated porous membrane, which separates the cell channels. We also introduce a cost-effective, easy to use pressure regulator to apply cyclic stretch across the porous membrane and the cells on it. The device thickness was reduced utilizing a cyclic olefin copolymer (COC) sheet as a lid, to allow for fluorescence imaging on the platform ('on-chip'). This platform, thus, enables live-cell imaging studies of cells or layers of cells exposed to simultaneous cyclic and/or shear stress or external triggers such as aerosolized particulates.

2 Materials and methods

2.1 Platform fabrication

2.1.1 Fabrication of photoresist-on-silicon masters for replica molding

Photoresist-on-silicon masters were created by photolithography with transparency photomasks (FineLine Imaging, Boulder, CO, USA). SU-8 2050 photoresist (Microchem Laboratory, Round Rock, TX, USA) was used for patterns of 150 µm tall vertical features on manifold and membrane masters. Photolithography with a second photomask and SU-8 2005 photoresist (Micochem Laboratory, Round Rock, TX, USA) were used for patterning 20 µm tall vertical micropillars (10 µm diameter and 40 µm center–center spacing) for the dual-layer lithography membrane master. All photoresist-on-silicon masters were developed in propylene glycol methyl ether acetate (PGMEA, Sigma-Aldrich, St. Louis, MO, USA). All photoresist-on-silicon masters were treated with (tridecafluoro-1,1,2,2-tetrahydrooctyl) trichlorosilane (Gelest, Morrisville, PA, USA) in a vacuum chamber for 4 h for easy release of soft lithographic replicas. Detailed fabrication method included in Sect. 1, Part A & B, of the SI.

2.1.2 Fabrication of 3 mm thick PDMS/COC microfluidic devices

A step-by-step photo/soft lithography microfluidic fabrication protocol is outlined in Sect. 1 of the supplementary information (SI). Polydimethylsiloxane (PDMS, SYLGARD 184, Dow Chemical Company, Midland, MI, USA) layers were fabricated using standard replica molding procedures by pouring a layer of PDMS onto a photoresist-on-silicon master with a total height ~ 3 mm thicker than the corresponding photoresist feature height to make the manifold layer. PDMS was spun onto a dual-layer membrane master with a total height ~ 10 µm thinner than the corresponding photoresist feature pillar height to make the membrane layer. For the manifold layer, PDMS was mixed with monomer: cross-linker ratio of 20:1 and cured at 70 °C for 1 h. For membrane layer, PDMS was mixed with monomer: cross-linker ratio of 10:1 and cured at 80 °C for 5 min.

These 3 mm thick platforms were assembled as follows: (i) PDMS was removed from the manifold layer master and holes were punched through the manifold layer creating inlet/outlet ports (ii) the resulting manifold layer assembly was aligned and irreversibly bonded to the PDMS membrane layer (iii) the bonded membrane and manifold layer were removed from the membrane master and a flat COC (TOPAS, Farmington Hills, MI, USA) sheet was bonded as the platform lid creating the complete platform. Inlet/outlet port holes were punched into the PDMS in step (i) using a blunt needle (BD PrecisionGlide Needle, BD, Franklin Lakes, NJ, USA). The irreversible PDMS–PDMS bond between the manifold layer and membrane layer in step (ii) was achieved by aligning the layers in direct contact and cooking at 70 °C for 2 h with weights. Finally, the COC–PDMS–PDMS assembly in step (iii) was reversibly or irreversibly bonded to an unpatterned COC substrate. Irreversible COC–PDMS bonding was achieved by activating the PDMS and COC surfaces using a plasma pretreatment with a plasma box (Harrick, Model PDC-001, Ithaca, NY, USA) and then heating at 70 °C for 15 min. Detailed fabrication method is included in Sect. 1, Parts A, B, and C, of the SI.

After preparation of the microfluidic masters was complete, 3 mm thick platforms were readily fabricated in 6 h. Each platform undergoes quality control testing before use in cell biology experiments. During quality control testing,

shear stress and cyclic stretch are applied to each platform. Platforms were used for cell biology experiments within a week of fabrication to minimize the effects of PDMS hardening over time. The most common avenues of failure are ripping of the porous membrane when removing membrane layer for membrane master, fluid leakage at the manifolds, or rupturing of sidewall between the cell and vacuum channels. Due to these avenues of failure, about half of the platforms fabricated could be used for experimentation. If platforms pass quality control testing, fully fabricated platforms are UV sterilized for 15–30 min before use in cell biology experiments.

2.1.3 Fabrication of 500 µm thick PDMS/COC microfluidic devices

PDMS layers were fabricated using standard replica molding procedures by spin-coating a layer of PDMS onto a photoresist-on-silicon master with a total height ~ 10 µm thicker than the corresponding photoresist feature height to make the manifold layer. PDMS was spun on to a dual-layer membrane master with a total height ~ 10 µm thinner than the corresponding photoresist feature pillar height to make the membrane layer. For the manifold layer, PDMS was mixed with monomer: cross-linker ratio of 5:1 and cured at 90 °C for 10 min. For membrane layer, PDMS was mixed with monomer: cross-linker ratio of 10:1 and cured at 70 °C for 5 min.

These 500 µm chips were assembled as follows: (i) a flat COC sheet with holes drilled to align with inlet/outlet ports was irreversibly bonded to a PDMS manifold layer (ii) a pre-cured PDMS block bonded to the manifold layer using uncured PDMS then holes were punched through the PDMS blocks and manifold layer creating channel inlet/outlet ports (iii) the resulting manifold layer assembly was aligned and irreversibly bonded to the PDMS membrane layer. Inlet/outlet port holes were drilled into the COC in step (i) using a drill (McMaster-Carr, Elmhurst, IL, USA). Permanent COC–PDMS layer assembly in step (i) was achieved by activating the surfaces using plasma pretreatment with a plasma box and then heating at 70 °C for 30 min. The irreversible PDMS–PDMS bond between the manifold layer and membrane layer in step (iii) was achieved by aligning the layers in direct contact and cooking at 70 °C for 2 h with weights. Finally, the COC–PDMS–PDMS assembly was reversibly or irreversibly bonded to an unpatterned COC substrate. Irreversible COC–PDMS bonding was achieved by activating the PDMS and COC surfaces using a plasma pretreatment with a plasma box and then heating at 70 °C for 15 min.

After preparation of microfluidic masters is complete, 500 µm thick platforms can be readily fabricated in 2–3 days. Each platform undergoes quality control testing before use in cell biology experiments. During quality control testing, shear stress and cyclic stretch are applied to each platform. Platforms were used for cell biology experiments within a week of fabrication to minimize the effects of PDMS hardening over time. Please note that the fabrication of a 500 µm platform is more laborious than a 3 mm thick platform. In addition, the 500 µm thick platforms have a lower pass rate during quality control testing compared to the 3 mm thick platforms. It is suggested to only fabricate thinner platforms for experiments that require imaging at 40 × magnification.

2.2 Pressure regulator development

The pressure regulator is fabricated using an Arduino Uno (#1141, Adafruit, New York, NY, USA), along with a data logging shield. The main components of the Arduino are a 3-port solenoid valve (LHDA0531115H, Lee Company, Franklin, TN, USA), pressure sensor, temperature sensor, and in-line filter. A heat sink surrounds the solenoid valve to prevent over heating during extended use. A SD card collects time stamped data records of temperature and pressure. The pressure sensor measures the pressure within the vacuum channels. Once fabricated, the solenoid valve is connected to vacuum channels with microbore polytetrafluoroethylene (PTFE) transfer tubing (Cole-Parmer, Vernon Hills, IL, USA). The temperature sensor records the ambient temperature surrounding the pressure regulator. The complete hardware and software design is included in Sect. 2 of the SI.

Measurements of linear distension were calculated by measuring the width of the porous membrane under cyclic stretch using images at points of full membrane expansion and relaxation. The change in porous membrane width resulted in linear distention percent change calculations (Eq. 1).

$$\%Linear\ Distension = \left(\frac{Width_{Expanded} - Width_{Relaxed}}{Width_{Relaxed}}\right) * 100 \quad (1)$$

2.3 Cell biology on the platform

2.3.1 Cell seeding in the platform

Endothelial cells (cell type dependent of shear stress or cyclic stretch experiment—see below) were grown to 80% confluence in a T75 flask with endothelial growth medium (dependent on cell type). 15 µg/mL of human fibronectin (Sigma-Aldrich, St. Louis, MO, USA) in phosphate buffered saline (PBS, Corning Inc., Corning, NY, USA) was incubated in the upper/lower cell channels for 15 min. After the fibronectin incubation, growth medium was manually pumped into the upper/lower channels to remove excess

fibronectin. Endothelial cells suspended in 150 µL of growth medium were manually pumped into upper channel. Following cell attachment to the PDMS surface for 2 h in a humidified incubator at 37 °C with 5% CO_2, growth medium with 1% penicillin–streptomycin (Corning Life Sciences, Tewksburg, MA, USA) was introduced into the upper channel using a syringe pump.

2.3.2 Application of shear stress on endothelial monolayers

Bovine aortic endothelial cells (BAECs, Cell Applications, Inc., San Diego, CA, USA) were seeded in the microfluidic platform (~ 3.3 million cells per 150 µL of medium). Following cell attachment to the PDMS for 2 h in a humidified incubator at 37 °C with 5% CO_2, bovine endothelial growth medium (Cell Application, Inc., San Diego, CA, USA) with 1% penicillin–streptomycin (Corning Life Sciences, Tewksburg, MA, USA) at a flow rate of 1 mL/hr was introduced into the upper channel using a peristaltic pump (MasterFlex L/S, Cole Parmer, Vernon Hills, IL, USA). BAECs were grown in the device for 2 days with continuous perfusion at 1 mL/hr of growth medium. On day 2, the flow rate was increased to 8 mL/hr, which generates a shear stress of 12 dynes/cm^2 across the BAECs seeded on the porous membrane. Shear stress and flow rate are related using the following equation, $\tau = 6\mu Q/H^2W$ (τ, fluid shear stress; µ, viscosity medium; Q, volume flow rate; H, channel height; W, channel width), developed for rectangular microfluidic channels.

2.3.3 Application of cyclic stretch on endothelial monolayers

Human pulmonary artery endothelial cells (HPAECs, Lonza, Morristown, NJ, USA) were seeded in the microfluidic platform (~ 1.5 million cells per 150 µL of medium). Following cell attachment to PDMS for 2 h in a humidified incubator at 37 °C with 5% CO_2, complete endothelial cell growth medium EGM-2 (Lonza, Morristown, NJ, USA) with 10% (v/v) FBS (Sigma-Aldrich, St. Louis, MO, USA) and 1% penicillin–streptomycin (Corning Life Sciences, Tewksburg, MA, USA) at a flow rate of 20 µL/hr was introduced into the upper channel using a syringe pump (Micro-Liter OEM Syringe Pump Modules, Harvard Apparatus, Holliston, MA, USA). In the incubator, HPAECs were grown in the device for 3 days with continuous 20 µL/hr flow of growth medium. On day 3, the pressure regulator was connected to the platform vacuum channels and cyclic stretch was applied across the cell channel for 2 h. During all cell biology experiments, the pressure regulator was placed outside of incubator to reduce contamination and was connected to platform vacuum channels, located in the incubator, using sterilized PTFE tubing.

2.3.4 Immunostaining and confocal imaging 'on-chip'

During all immunostaining steps fluids were manually syringed into upper/lower channels. Samples were fixed using 2% paraformaldehyde (Fisher, Hampton, NH, USA) in PBS for 15 min at 37 °C. Cells were permeabilized by 0.1% (v/v) Triton X-100 in PBS for 10 min at 37 °C, and non-specific antibody binding blocked by 1% (w/v) BSA in PBS for 1 h. Fluorescent staining was performed for 1 h with 4',6-diamidino-2-phenylindole, dihydrochloride (DAPI, 1:1000 dilution) to stain the nuclei and Rhodamine Phalloidin (1:200 dilution) to image F-actin. Samples were mounted in Fluoromount-G (SouthernBiotech, Birmingham, AL, USA) 'on-chip', and were stored at 4 °C until imaging. Samples were imaged 'on-chip' using a confocal microscope Zeiss LSM 880 (Carl Zeiss AG, Oberkochen, Germany) with a 10× objective (EC Plan-Neofluar 10x/0.30, Carl Zeiss AG, Oberkochen, Germany), 20× objective (Plan-Apochromat 20x/0.8, Carl Zeiss AG, Oberkochen, Germany), and/or 40× objective (C-Apochromat 40x/1,2 W Korr, Carl Zeiss AG, Oberkochen, Germany). When capturing each single layer image for analysis, the microscope was focused on the cross section with clear definition in F-actin. Due to the nature of fixing and immunostaining 'on-chip', a new microfluidic platform was used for each cell biology experiment.

3 Results and discussion

3.1 Platform design

Our goal was to design a platform that incorporated the following attributes: (a) porous membrane between channels; (b) able to apply a physiologically relevant shear stress; (c) able to apply a physiologically relevant cyclic stretch; and (d) allowing for cell imaging on the platform. To incorporate these attributes, the design shown in Fig. 1A was used. Dual-layer lithography was utilized to create masters that result in a microfluidic porous membrane (design attribute a) between channels. Syringe pumps are used to apply shear stress (design attribute b) over endothelial monolayers mimicking blood flow within blood vessels. Alternation of the pressure in the microfluidic channels flanking the cell channel results in cyclic stretch of the porous membrane (design attribute c). This cyclic stretch mimics physiological breathing within the lung alveoli. A pressure regulator was specifically developed for this project to produce periodic expansion and contraction patterns in the vacuum channels. The use of COC enabled us to reduce the thickness of the platform to allow for cell imaging 'on-chip' (design attribute d). The overall platform is formed through assembly of three components: a manifold fluidic layer, a porous membrane

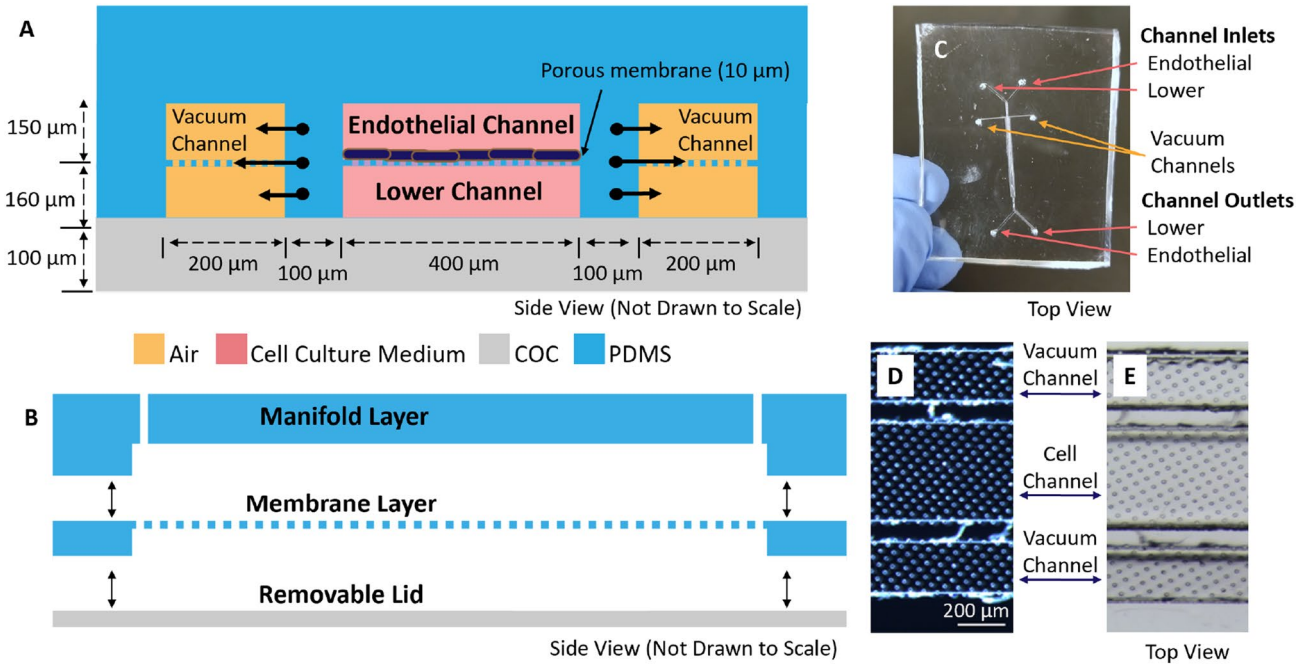

Fig. 1 Microfluidic platform **a** Cross-section schematic of the 3 mm thick microfluidic platform with established endothelial monolayer. The microfluidic platform has a 400 µm cell channel and two flanking vacuum channels separated by a 100 µm PDMS walls. Endothelial cells seeded on a stretchable, porous membrane experience linear distension when cyclic vacuum is applied to the vacuum channels. During cyclic stretch, shear stress can also be applied over the endothelial cells with cell culture medium flow through the cell channels using syringe/peristaltic pumps. **b** Soft-lithography fabrication schematic of the manifold layer, membrane layer, and removable COC lid that are bonded to create the platform. **c** Photograph of the fully assembled 3 mm thick microfluidic platform. **d** Dual-layer membrane master used to create 10 µm pores (40 µm center-to-center distance) on the membrane layer. (e) Close-up of the porous membrane and the cell and vacuum channels in a fully assembled platform

fluidic layer, and a COC lid (Fig. 1B). The fully assembled microfluidic platform can be seen in Fig. 1C.

3.1.1 Dual-layer photolithography for porous membrane layer fabrication

Instead of using demanding techniques that require a skilled operator, such as deep reactive ion etching, to fabricate a stretchable, porous membranes (Stucki et al. 2015; Huh et al. 2013), we take advantage of dual-layer lithography to fabricate an organ-on-a-chip platform with a stretchable porous membrane (Fig. S1). Figures S1, S2, & S3, provide detailed schematics of the entire platform fabrication protocol. The dual-layer membrane master is comprised of 20 µm tall micropillars that are 10 µm in diameter, positioned on top of the cell and vacuum channels (Fig. 1D). This master can be reused for replication at least 50 times. The minimum micropillar diameter that can be achieved using this dual-layer lithography method is 7 µm. This minimum feature size is governed by the plot resolution (dots per inch) used to print the micropillar mask on transparency film. During traditional photolithography, exposed photoresist is developed by placing the exposed substrate in a beaker with PGMEA and agitated until development is complete. This method leads to the collapse of the 10 µm micropillar array. To prevent the micropillars from collapsing, we place the substrate—after dual exposure—upside down in the PGMEA solution. In this manner, any dissolving SU-8 photoresist will move away from the silicon wafer, due to a difference in density with the PGMEA, and settle on the bottom of the beaker. This approach prevents the posts from being covered with SU-8 residue and collapsing against each other. Once fully developed, this dual-layer membrane master is removed from the PGMEA solution, air dried while still upside down, hard-baked right side up, and silanized. Now, the dual-layer membrane master can be replicated in PDMS via spin-coating and subsequent annealing, to yield the contours of the cell and vacuum channels as well as the membrane with 10 µm diameter pores and center–center pore spacing of 40 µm (Fig. 1E). The desired PDMS (10:1 ratio) thickness of the porous, membrane layer was determined by the need to completely cover the channels (~ 150 µm height) while still exposing the top of the micropillars (~ 20 µm height). This desired PDMS thickness was ~ 160 µm and was achieved at a spin speed of 850 RPM. The stretchable, porous membrane in the cell channel provides support to seeded cells that then

can grow to confluence, while at the same time allowing for cell–cell communication between cell layers placed on opposite sides of the membrane. With an established soft lithography fabrication protocol, through-holes in the membrane were tested by pumping dyed water in the upper channel and undyed water in the lower channel. Diffusion across the pores was visually checked by observing the presence of dye in the outlet of the lower channel. Once the optimized fabrication protocol was established, the same PDMS ratio (10:1) and spin speed (850 RPM) were used to insure reproducibility of porous membrane. After fabrication of reusable photolithography masters, production of 3 mm thick microfluidic platforms takes only 6 h, with half of that time being consumed by waiting for baking and bonding steps.

More in general, we believe that this dual-layer lithography technique including the upside down development step can be utilized broadly to create molds for fabrication of thin, porous PDMS membranes. Creating porous, stretchable membranes has been a challenge in the microfluidic fabrication community, to date, typically requiring more demanding techniques such as deep reactive ion etching. Work by Zamprogno et al. addresses this issue by creating stretchable membranes out of biodegradable collagen and elastin (Zamprogno et al. 2021). Due to difficulties in fabricating porous, stretchable membranes, polyester membranes can also be used as porous, non-stretchable membranes in microfluidic platforms not requiring cyclic stretch conditions (Nalayanda et al. 2009).

3.1.2 Application of physiologically relevant shear stress

Vascular endothelial cell structure and physiology is influenced by shear stress the cells experience in the vasculature due to blood flow. The design of our platform includes two horizontally stacked rectangular channels ($H = 150$ µm, $W = 400$ µm, $L = 34.3$ mm)–an endothelial channel and a lower channel. Both channels have their own inlet and outlet manifold. For the purposes of our biological experiments, cell culture medium is flown through the endothelial channel to apply shear stress to the endothelial cells. A constant flow rate of cell culture medium was delivered using a peristaltic pump. The equation $\tau = 6\mu Q/H^2W$ was used to relate flow rate to fluid shear stress over cells in the endothelial channel. Using a flow rate of ~ 8 mL/hr exerts a wall shear stress of 12 dynes/cm^2, which is a physiologically relevant shear stress (Tzima et al. 2005).

3.1.3 Use of portable pressure regulator for cyclic stretch

Our next goal was to develop the ability to apply cyclic stretch to the porous membrane and the cells attached to it, mimicking the expansion/contraction of the lung alveoli and endothelial bilayer. This is achieved by varying the pressure in the vacuum channels, thereby causing periodic expansion/contraction, resulting in linear distension of the porous membrane.

Previously reported lung-on-a-chip platforms often utilize high cost, market available pressure regulators to produce cyclic stretch on lung-on-a-chip platforms (Huh et al. 2013; Peel et al. 2019). We pursued an alternative, more accessible approach: development of a portable pressure regulator comprised of affordable off-the-shelve electronic and pneumatic actuation parts (Fig. 2A). For the electronics and controls, we chose an Arduino-based design connected to a solenoid valve, pressure sensor, temperature sensor, in-line filter, and SD card. The result is a pressure regulator that is programmable and can apply periodically fluctuating pressures to our microfluidic platform. Indeed by fine-tuning the programming, we can cycle the pressure (Fig. 2B) with amplitudes and periods that mimic human breathing (Albanese et al. 2016).

The Arduino hardware and software design, including the Arduino circuit diagram (Fig. S4) and code programmed on the Arduino, are outlined in Sect. 2 of the SI. The code can be adjusted to apply desired pressure cycles. To do so, the 'setPressure' array, consisting of 256 pressure set points, can be adjusted to achieve desired period/amplitude of pressure variation in the vacuum channels. This versatility is beneficial because adjusting the PDMS crosslinker ratios or channel height of the platform will require adjusting the pressure set points to achieve desired linear distension across the porous membrane. For example, on

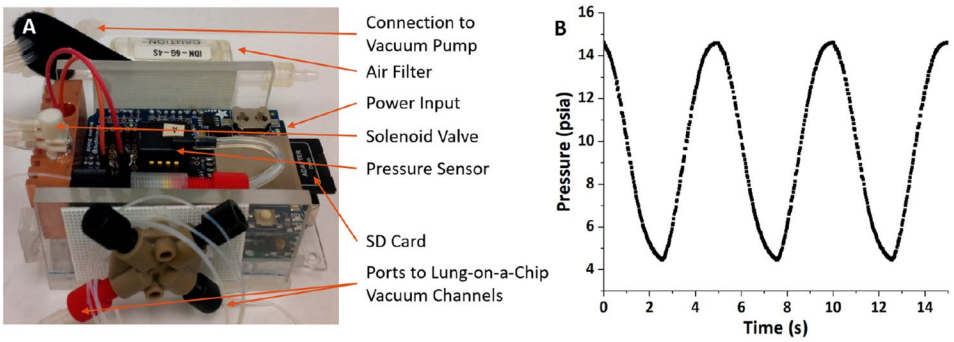

Fig. 2 Pressure regulator **a** Image of the portable pressure regulator and its components. **b** Pressure vs. time generated by the pressure regulator, here resulting in 6.2% linear distention of the platform's porous membrane, in the range of physiologically relevant cyclic stretch

our platform, we were able to achieve different percentages of linear distension across the porous membrane ranging from 1.7% ± 0.3 to 16.4% ± 1.3 by varying the pressure set points at a frequency of 0.22 Hz. These levels of linear distension correlate with pressure set points ranging from 17.3 to 14.7 (ambient pressure) psi and 15.1 to 14.7 psi, respectively. The range of linear distension achieved using our pressure regulator is consistent with physiologically relevant linear distension occurring within in vivo lung alveoli (Birukov et al. 2003). The cost of the fully assembled pressure regulator equals about $500. This is a 70% reduction in cost compared to pressure regulators used with existing lung-on-a-chip platforms (Huh et al. 2013). In addition, our pressure regulator has successfully run for seven straight days. The pressure regulator enables sinusoidal contraction and relaxation of the vacuum channels resulting in a 5.1% ± 0.3 linear distension of the porous membrane in the cell channel (Movie S1 in the SI). During the application of sinusoidal vacuum, the flimsy membrane in the vacuum channels deform as the 100 µm PDMS side walls expand outward. As a result, linear distention of the porous membrane in the cell channels is not impacted by the presence of the membrane in the vacuum channels. By changing the design of the cell channel compartment, one could also expose cells to biaxial stretching. The Young's modulus of PDMS is generally regarded as dimensionally independent in bulk quantities and is reported to be 2.6 MPa for 10:1 PDMS (Wang et al. 2014). At membrane thicknesses of less than 200 µm, the PDMS mechanical properties become thickness dependent. Liu et al. report a 10:1 PDMS thickness of 50 µm having a Young's modulus of 1.4 MPa (Liu et al. 2009).

3.1.4 In situ imaging on the platform

3.1.4.1 Enabling in situ imaging PDMS scatters light during confocal imaging. As a result, images are often blurry when taken on thick microfluidic platforms. Our platform design reduces the device thickness to enable clear microscopic imaging 'on-chip'. Reducing the thickness of microfluidic platforms is traditionally limited by the inability to handle thin layers of PDMS as they easily deform and flex upon handling. By utilizing a thin sheet of clear plastic, COC, as the lid of the platform (Fig. 1B), we reduced the platform thickness while maintaining platform rigidity (Fig. S1, S2, & S3). The thickness of the assembled platforms, 3 mm and 500 µm, are compatible with high-resolution imaging techniques (Wang et al. 2008; Khvostichenko et al. 2013; Guha et al. 2012). Platform compatibility to high-resolution imaging was informed by the reported working distance of microscope objectives. While each objective's working distance is different, we determined that cells seeded on the porous membrane, positioned about ~ 260 µm from the base of the 3 mm and 500 µm thick platforms could be imaged in an inverted microscope with a Plan-Apochromat 20x/0.8 M27 objective that reports a working distance of 0.55 mm. Cells seeded on the porous membrane of a 500 µm thick platform, could also be imaged with a C-Apochromat 40x/1,2 W Korr objective that reports a working distance of 0.28 mm.

3.1.4.2 Exposing cells to aerosolized particulates Another attribute of using a COC lid is that the lid can be bonded reversibly or irreversibly to the platform's PDMS. Native COC can be reversibly bonded and then removed from PDMS. In cases where irreversible bonding between COC and PDMS is desired, oxygen plasma bonding or covalent amine epoxy chemistry can be used. The reversibility of the bond between COC and PDMS provides an opportunity for organ-on-a-chip experiments where access to the cells is needed at some point. For example, the removable COC lid can be removed from the platform to expose differentiated lung epithelium, enabling studies that explore the effect of aerosolized particulates on cell function (Sect. 1, Part C, of the SI & Fig. S3). Traditionally, laboratories have used nebulizers to aerosolize particulates over cell culture experiments in transwell plates (Röhm et al. 2017; Lenz et al. 2009, 2014). Whereas, exposing cell culture samples in lung-on-a-chip platforms to particulates requires the introduction of particulates suspended in a liquid stream (Huh et al. 2010) or the introduction of airborne particulates via an ancillary gas injection system (Benam et al. 2016a; Elias-Kirma et al. 2020). Work by Artzy-Schnirman et al. makes an effort to utilize an aerosol deposition system with lung-on-a-chip platforms (Artzy-Schnirman et al. 2019). In summary, the transition from transwells to lung-on-a-chip platforms requires the use of more complex particulate exposure setups. Our microfluidic platform addressed this limitation using a reversibly bonded COC lid allowing for aerosol exposure using a nebulization system—traditionally used with transwell plate experiments.

3.2 Validating platform functionality

3.2.1 Imaging 'on-chip'

To validate the subcellular imaging capabilities in our platform, we seeded endothelial cells on the porous membrane in the endothelial channel and immunostained for nuclei and actin filaments. After two days in culture, the bovine aortic endothelial cells (BAECs) were fixed and immunostained for F-actin and nuclei 'on-chip'. Imaging was also performed using confocal microscopy (Fig. S5). Endothelial cells seeded on the porous membrane in the 500 µm thick

platform were imaged using an objective up to a 40x (Fig. S5B). At this magnification, clear cortical actin fibers can be seen in the form of a layer of crosslinked proteins on the inner face of the cell membrane. Somewhat unexpectedly, a layer of BAECs was also observed on the bottom of the lower channel (Fig. S6). Upon future research, migration through the 10 µm membrane pores is consistent with observations by Discher et al. and Lammerding et al. that cells can migrate through narrow pores (Pfeifer et al. 2019; Krause et al. 2019; Irianto et al. 2017). An inability to achieve consistent cell attachment during seeding and inconsistency when developing confluent monolayer on the porous membrane, is an inherent limitation of cell growth on our microfluidic platform. This variability could potentially be attributed to the use of primary cells lines, resulting in more variability compared to immortalized cell lines. This would warrant further optimization of the biological studies with specific cell lines.

In typical efforts to get high-definition imaging of organ-on-a-chip samples, cell culture samples are removed from platforms and imaged on glass microscope slides (Benam et al. 2016b). Although this is effective, it adds complexity to imaging and is not conducive to live-cell imaging. Efforts have been taken to optimize 'on-chip' imaging with innovative fabrication procedures (Stucki et al. 2015, 2018; Zamprogno et al. 2021), simplified designs (Yang et al. 2018; Humayun et al. 2018; Li et al. 2014), and the adoption of automated imaging (Peel et al. 2019). With our platform offering the option to image 'on-chip', we next focused on observing the morphological effects of physiologically relevant shear stress and cyclic stretch on monolayers of endothelial cells.

3.2.2 Simultaneous mechanical and hydrodynamic perturbations

Previously, parallel plate flow chambers have been used to apply fluid shear stress across cells (Tzima et al. 2005; Levesque and Nerem 1985). Separately, commercial bioreactors that can apply cyclic/static strain (Birukov et al. 2003; Birukova et al. 2008a, 2008b; Liu et al. 2007) and equiaxial stretchers (Dan et al. 2016) have been used to apply mechanical stretch across cells. One key advantage of organ-on-a-chip platforms, such as the one reported here, is their ability to apply simultaneous mechanical and hydrodynamic forces experienced by cells in vivo.

3.2.2.1 Shear stress Bovine aortic endothelial cells (BAECs) were seeded on one side of the platform's porous membrane and grown to a confluent monolayer. BAECs where chosen for endothelial imaging because they have been shown to align with flow at shear stress values between 12 and 50 dynes/cm^2 (Sprague et al. 1987; Ives et al. 1986; Tzima et al. 2005). On day 2, we applied shear stress, at 12 dynes/cm^2, across the monolayer of BAECs for 16 h using syringe pumps. Confocal imaging 'on-chip' reveals the lack of uniform BAEC actin alignment with the direction of flow across the entire platform (Fig. 3 A and B). Figure 3A was obtained using a 10×objective and Fig. 3B was obtained using a 20×objectives. Both images were obtained along the length of the same microfluidic platform. This result was compared to the control condition—without exposure to shear stress—in Figure S5. In the control, BAECs were seeded on the platform's porous membrane and grown for 2 days before immunostaining and image 'on-chip'. While

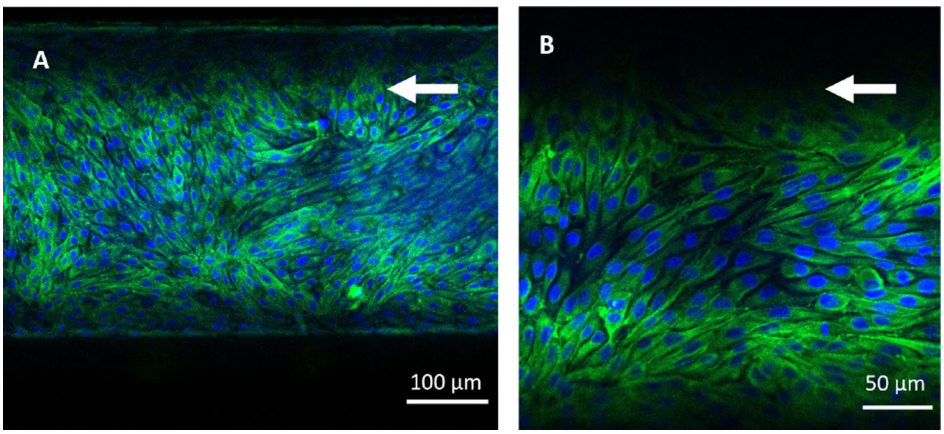

Fig. 3 'On-chip' imaging following shear stress exposure Immunofluorescence images of BAECs after exposure to shear stress on the microfluidic platform imaged using **a** 10×and **b** 20×objectives (actin: green and nuclei: blue). BAECs were seeded on the porous membrane of a platform (thickness: 3 mm). After 2 days of cell growth under a steady supply of 20 µL/hr of medium, 12 dynes/cm^2 of cell medium was flown over the cells for 16 h. BAECs were immunostained and imaged at the porous membrane focal plane with confocal microscopy. The arrows indicate the direction of flow

this is a preliminary biological experiment, the lack of alignment could be due to the uneven topography of the 10 µm thick, porous membrane impacting endothelial cell focal adhesions. BAECs, imaged at the endothelial channel ceiling, presented cell alignment with the direction of flow at varying regions along the length of the entire platform (Fig. S7A). Cell alignment was not uniform across the length of the entire endothelial channel ceiling (Fig. S7B). This could indicate that the topographical heterogeneity and flexibility of the porous membrane could result in inconsistent shear stress within the walls of the endothelial cell channel. Other groups have also reported challenges in achieving uniform endothelial alignment in channels under flow (Wong and Simmons 2019).

While imaging 'on-chip', we encountered a problem possibility associated with the current platform design. In Fig. 3, the actin and nuclei are not in focus across the entire monolayer. This is evidence that the PDMS membrane is not flat, but slightly wavey across the length of the porous membrane. The membrane variability translates to different regions being in and out of focus within the focal plane of each objective. Compared to the platform used in Fig. 3, the platforms used in Fig. 4 and S5 have a flat porous membrane; as a result, the endothelial monolayers in Fig. 4 and S5 are in focus within the objective focal plane. The waviness of the porous membrane is an inherent limitation of the fabrication process and arises when bonding the manifold layer to the membrane layer.

3.2.2.2 Cyclic stretch Human pulmonary artery endothelial cells (HPAECs) were seeded on the porous membrane and grown to confluence. HPAECs where used for this imaging study because their mechanosensory response to cyclic stretch is well studied (Birukov et al. 2003). In the presence of physiologically relevant cyclic stretch, HPAEC actin fibers align perpendicular to the direction of linear distension (Birukov et al. 2003). On day 3, cyclic stretch at $5.1\% \pm 0.3$ was applied across the monolayer of HPAECs for 2 h at a frequency of 0.22 Hz using the portable pressure regulator. Confocal imaging 'on-chip' visualized HPAEC actin organization, along the length of the same microfluidic platform, using 10x (Fig. 4A) and 20x (Fig. 4B) objectives. Actin fibers exposed to cyclic stretch oriented perpendicular to the stretch direction. This result was compared to the control condition—without exposure to cyclic stretch—in Figure S8. In the control, HPAECs were seeded on the microfluidic platform's porous membrane and grown for 3 days before immunostaining and image 'on-chip'.

Overall, this platform has the capability to pair the pressure regulator and syringe/peristaltic pump to induce cyclic stretch and/or shear stress to mimic the mechanical and hydrodynamic forces associated with breathing and blood flow. The biological complexity of the platform can be expanded to include co-cultures of airlifted epithelial cells and vascular endothelial cells, creating a lung-on-a-chip platform. Functional assays can also be performed such as cell viability, permeability, cytokine secretions, etc. One can also take advantage of the platform's reversible bonding between COC and PDMS to enable studies requiring exposure of the cell culture samples seeded within the platform to aerosolized particulates (*e.g.*, to study the effect of air pollution). This platform may be used as a tool to complete subcellular, live-cell imaging of healthy or diseased lung tissue, *e.g.*, in the presence or absence of certain pollutants or pharmaceuticals.

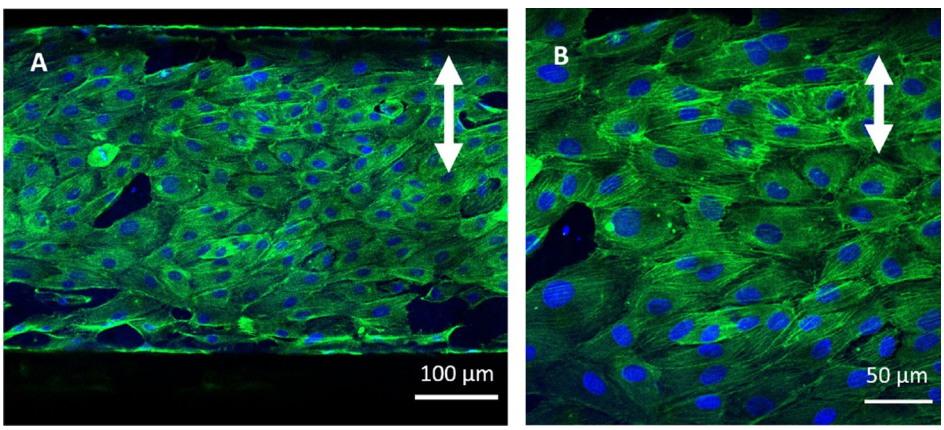

Fig. 4 'On-chip' imaging following cyclic stretch exposure Immunofluorescence images of HPAECs after exposure to cyclic stretch on the microfluidic platform imaged using **a** 10× and **b** 20× objectives (actin: green and nuclei: DAPI blue). HPAECs were seeded on the porous membrane of a platform (thickness: 3 mm). After 3 days of cell growth under a steady flow of medium at 20 µL/hr, 5.1% linear distension was applied to the porous membrane for 2 h, using the pressure regulator. HPAECs were immunostained and imaged at the porous membrane focal plane with confocal microscopy. The arrows indicate the direction of cyclic stretch

4 Conclusion

Limited access to pressure regulators and the need for advanced fabrication techniques to fabricate stretchable, porous membranes has limited the adoption of organ-on-a-chip technology with shear stress and cyclic stretch capabilities by the biomedical community. To address these limitations, we report the development of an accessible microfluidic platform that recapitulates the physiological environment of cells exposed to shear and/or cycle stretch with in situ imaging capabilities. Our platform takes advantage of traditional photo/soft lithography techniques and Arduino technology to reduce equipment requirements. After preparation of microfluidic masters, platforms can be readily fabricated in 6 h. The platform design exploits a stretchable, porous PDMS membrane that is fabricated using dual-layer lithography. The platform can be operated with an accessible pressure regulator that enables application of physiologically relevant cyclic stretch in the platform. Furthermore, use of a transparent COC sheet as a lid decreases the platform thickness, enabling subcellular imaging 'on-chip'. Here, we used confocal imaging to demonstrate being able to obtain immunofluorescent images of endothelial monolayers 'on-chip' following the application of physiologically relevant shear stress and cyclic stretch.

Supplementary Information The online version contains supplementary material available at https://doi.org/10.1007/s10404-022-02619-y.

Acknowledgements This work is supported by the National Institutes for Health under grants R21-HL129115-02 and F31 ES29833-1, and the National Science Foundation under grant 1735252. We gratefully appreciate the support from the staff of the Core Facilities at the Carl R. Woese Institute for Genomic Biology and the School of Chemical Sciences Machine Shop at the University of Illinois at Urbana-Champaign, USA.

Author contributions WES, ASP, JMS, and JJW collaborated in designing the fabrication procedure. ASP developed the pressure regulator and protocol for dual-layer lithography. WES and TAL fabricated the microfluidic platforms. WES completed 'on-chip' imaging of endothelial cells. WES wrote the manuscript. PJAK and DEL oversaw all experimental work and subsequent analysis. All authors reviewed the manuscript.

Funding This work is supported by the National Institutes for Health under grants R21-HL129115-02 and F31 ES29833-1, and the National Science Foundation under grant 1735252.

Data availability The data that support the findings of this study are available within the article and its supplementary material.

Code availability See the supplementary information for the Arduino-based pressure regulator code.

Declarations

Conflict of interest The authors have no conflicts of interest to declare that are relevant to the content of this article.

References

Albanese A, Cheng L, Ursino M, Chbat NW (2016) An integrated mathematical model of the human cardiopulmonary system: model development. Am J Physiol-Heart Circ Physiol 310:H899–H921. https://doi.org/10.1152/ajpheart.00230.2014

Artzy-Schnirman A, Hobi N, Schneider-Daum N, Guenat OT, Lehr C-M, Sznitman J (2019) Advanced in vitro lung-on-chip platforms for inhalation assays: from prospect to pipeline. Eur J Pharm Biopharm 144:11–17. https://doi.org/10.1016/j.ejpb.2019.09.006

Artzy-Schnirman A, Arber Raviv S, DoppeltFlikshtain O, Shklover J, Korin N, Gross A, Mizrahi B, Schroeder A, Sznitman J (2021) Advanced human-relevant in vitro pulmonary platforms for respiratory therapeutics. Adv Drug Deliv Rev. https://doi.org/10.1016/j.addr.2021.113901

Beißner N, Lorenz T, Reichl S (2016) Organ on Chip. In: Dietzel A (ed) Microsystems for Pharmatechnology: Manipulation of Fluids, Particles, Droplets, and Cells. Springer International Publishing, Cham, pp 299–339

Benam KH, Novak R, Nawroth J, Hirano-Kobayashi M, Ferrante TC, Choe Y, Prantil-Baun R, Weaver JC, Bahinski A, Parker KK, Ingber DE (2016a) Matched-comparative modeling of normal and diseased human airway responses using a microengineered breathing lung chip. Cell Syst 3:456-466.e454. https://doi.org/10.1016/j.cels.2016.10.003

Benam KH, Villenave R, Lucchesi C, Varone A, Hubeau C, Lee H-H, Alves SE, Salmon M, Ferrante TC, Weaver JC, Bahinski A, Hamilton GA, Ingber DE (2016b) Small airway-on-a-chip enables analysis of human lung inflammation and drug responses in vitro. Nat Meth 13:151–157. https://doi.org/10.1038/nmeth.3697

Bhatia SN, Ingber DE (2014) Microfluidic organs-on-chips. Nat Biotechnol 32:760. https://doi.org/10.1038/nbt.2989

Birukov KG, Jacobson JR, Flores AA, Ye SQ, Birukova AA, Verin AD, Garcia JGN (2003) Magnitude-dependent regulation of pulmonary endothelial cell barrier function by cyclic stretch. Am J Physiol - Lung Cell Mole Physiol 285:L785–L797. https://doi.org/10.1152/ajplung.00336.2002

Birukova AA, Moldobaeva N, Xing J, Birukov KG (2008a) Magnitude-dependent effects of cyclic stretch on HGF- and VEGF-induced pulmonary endothelial remodeling and barrier regulation. Am J of Physiol Lung Cell Mole Physiol 295:L612–L623. https://doi.org/10.1152/ajplung.90236.2008

Birukova AA, Rios A, Birukov KG (2008b) Long-term cyclic stretch controls pulmonary endothelial permeability at translational and post-translational levels. Exp Cell Res 314:3466–3477. https://doi.org/10.1016/j.yexcr.2008.09.003

Charbonier FW, Zamani M, Huang NF (2019) Endothelial cell mechanotransduction in the dynamic vascular environment. Adv Biosyst. https://doi.org/10.1002/adbi.201800252

Dan A, Huang RB, Leckband DE (2016) Dynamic imaging reveals coordinate effects of cyclic stretch and substrate stiffness on endothelial integrity. Ann Biomed Eng 44:3655–3667. https://doi.org/10.1007/s10439-016-1677-4

Dudek SM, Garcia JGN (2001) Cytoskeletal regulation of pulmonary vascular permeability. J Appl Physiol 91:1487–1500. https://doi.org/10.1152/jappl.2001.91.4.1487

Elias-Kirma S, Artzy-Schnirman A, Das P, Heller-Algazi M, Korin N, Sznitman J (2020) In situ-Like aerosol inhalation exposure for cytotoxicity assessment using airway-on-chips platforms. Front Bioeng Biotechnol 8:91. https://doi.org/10.3389/fbioe.2020.00091

Guha S, Perry SL, Pawate AS, Kenis PJA (2012) Fabrication of X-ray compatible microfluidic platforms for protein crystallization. Sens Actuators, B Chem 174:1–9. https://doi.org/10.1016/j.snb.2012.08.048

Hahn C, Schwartz MA (2009) Mechanotransduction in vascular physiology and atherogenesis. Nat Rev Mol Cell Biol 10:53–62. https://doi.org/10.1038/nrm2596

Huh D, Matthews BD, Mammoto A, Montoya-Zavala M, Hsin HY, Ingber DE (2010) Reconstituting Organ-Level lung functions on a chip. Science 328:1662–1668. https://doi.org/10.1126/science.1188302

Huh D, Leslie DC, Matthews BD, Fraser JP, Jurek S, Hamilton GA, Thorneloe KS, McAlexander MA, Ingber DE (2012a) A Human disease model of drug toxicity-induced pulmonary edema in a lung-on-a-chip microdevice. Sci Translat Med. https://doi.org/10.1126/scitranslmed.3004249

Huh D, Torisawa Y-s, Hamilton GA, Kim HJ, Ingber DE (2012b) Microengineered physiological biomimicry: Organs-on-Chips. Lab Chip 12:2156–2164. https://doi.org/10.1039/C2LC40089H

Huh D, Kim HJ, Fraser JP, Shea DE, Khan M, Bahinski A, Hamilton GA, Ingber DE (2013) Microfabrication of human organs-on-chips. Nat Protocols 8:2135–2157. https://doi.org/10.1038/nprot.2013.137

Humayun M, Chow C-W, Young EWK (2018) Microfluidic lung airway-on-a-chip with arrayable suspended gels for studying epithelial and smooth muscle cell interactions. Lab Chip 18:1298–1309. https://doi.org/10.1039/C7LC01357D

Irianto J, Xia Y, Pfeifer CR, Athirasala A, Ji J, Alvey C, Tewari M, Bennett RR, Harding SM, Liu AJ, Greenberg RA, Discher DE (2017) DNA damage follows repair factor depletion and portends genome variation in cancer cells after pore migration. Curr Biol 27:210–223. https://doi.org/10.1016/j.cub.2016.11.049

Ives CL, Eskin SG, McIntire LV (1986) Mechanical effects on endothelial cell morphology: In vitro assessment. In Vitro Cell Dev Biol 22:500–507. https://doi.org/10.1007/BF02621134

Jain A, Barrile R, van der Meer A, Mammoto A, Mammoto T, De Ceunynck K, Aisiku O, Otieno M, Louden C, Hamilton G, Flaumenhaft R, Ingber D (2018) Primary human lung alveolus-on-a-chip model of intravascular thrombosis for assessment of therapeutics. Clin Pharmacol Ther 103:332–340. https://doi.org/10.1002/cpt.742

Khvostichenko DS, Kondrashkina E, Perry SL, Pawate AS, Brister K, Kenis PJA (2013) An X-ray transparent microfluidic platform for screening of the phase behavior of lipidic mesophases. Analyst 138:5384–5395. https://doi.org/10.1039/c3an01174g

Krause M, Yang FW, Te Lindert M, Isermann P, Schepens J, Maas RJA, Venkataraman C, Lammerding J, Madzvamuse A, Hendriks W, Te Riet J, Wolf K (2019) Cell migration through three-dimensional confining pores: speed accelerations by deformation and recoil of the nucleus. Philos Trans R Soc Lond B Biol Sci 374:20180225. https://doi.org/10.1098/rstb.2018.0225

Lenz AG, Karg E, Lentner B, Dittrich V, Brandenberger C, Rothen-Rutishauser B, Schulz H, Ferron GA, Schmid O (2009) A dose-controlled system for air-liquid interface cell exposure and application to zinc oxide nanoparticles. Part Fibre Toxicol 6:32. https://doi.org/10.1186/1743-8977-6-32

Lenz AG, Stoeger T, Cei D, Schmidmeir M, Semren N, Burgstaller G, Lentner B, Eickelberg O, Meiners S, Schmid O (2014) Efficient bioactive delivery of aerosolized drugs to human pulmonary epithelial cells cultured in air-liquid interface conditions. Am J Respir Cell Mol Biol 51:526–535. https://doi.org/10.1165/rcmb.2013-0479OC

Levesque MJ, Nerem RM (1985) The elongation and orientation of cultured endothelial cells in response to shear stress. J Biomech Eng 107:341–347. https://doi.org/10.1115/1.3138567

Li L, Yang Y, Shi X, Wu H, Chen H, Liu J (2014) A microfluidic system for the study of the response of endothelial cells under pressure. Microfluid Nanofluid 16:1089–1096. https://doi.org/10.1007/s10404-013-1275-9

Liu WF, Nelson CM, Tan JL, Chen CS (2007) Cadherins, RhoA, and Rac1 are differentially required for stretch-mediated proliferation in endothelial versus smooth muscle cells. Circ Res 101:e44–e52. https://doi.org/10.1161/CIRCRESAHA.107.158329

Liu M, Sun J, Sun Y, Bock C, Chen Q (2009) Thickness-dependent mechanical properties of polydimethylsiloxane membranes. J Micromech Microeng. https://doi.org/10.1088/0960-1317/19/3/035028

Malek AM, Alper SL, Izumo S (1999) Hemodynamic Shear stress and its role in atherosclerosis. JAMA 282:2035–2042. https://doi.org/10.1001/jama.282.21.2035

Meghani N, Kim KH, Kim SH, Lee SH, Choi KH (2020) Evaluation and live monitoring of pH-responsive HSA-ZnO nanoparticles using a lung-on-a-chip model. Arch Pharm Res 43:503–513. https://doi.org/10.1007/s12272-020-01236-z

Nalayanda DD, Puleo C, Fulton WB, Sharpe LM, Wang T-H, Abdullah F (2009) An open-access microfluidic model for lung-specific functional studies at an air-liquid interface. Biomed Microdevice 11:1081. https://doi.org/10.1007/s10544-009-9325-5

Pattanayak P, Singh SK, Gulati M, Vishwas S, Kapoor B, Chellappan DK, Anand K, Gupta G, Jha NK, Gupta PK, Prasher P, Dua K, Dureja H, Kumar D, Kumar V (2021) Microfluidic chips: recent advances, critical strategies in design, applications and future perspectives. Microfluid Nanofluid 25:99. https://doi.org/10.1007/s10404-021-02502-2

Peel S, Corrigan AM, Ehrhardt B, Jang K-J, Caetano-Pinto P, Boeckeler M, Rubins JE, Kodella K, Petropolis DB, Ronxhi J, Kulkarni G, Foster AJ, Williams D, Hamilton GA, Ewart L (2019) Introducing an automated high content confocal imaging approach for Organs-on-Chips. Lab Chip 19:410–421. https://doi.org/10.1039/C8LC00829A

Pfeifer CR, Irianto J, Discher DE (2019) Nuclear Mechanics and Cancer Cell Migration. In: La Porta CAM, Zapperi S (eds) Cell Migrations: Causes and Functions. Springer International Publishing, Cham, pp 117–130

Röhm M, Carle S, Maigler F, Flamm J, Kramer V, Mavoungou C, Schmid O, Schindowski K (2017) A comprehensive screening platform for aerosolizable protein formulations for intranasal and pulmonary drug delivery. Int J Pharm 532:537–546. https://doi.org/10.1016/j.ijpharm.2017.09.027

Sprague EA, Steinbach BL, Nerem RM, Schwartz CJ (1987) Influence of a laminar steady-state fluid-imposed wall shear stress on the binding, internalization, and degradation of low-density lipoproteins by cultured arterial endothelium. Circulation 76:648–656. https://doi.org/10.1161/01.cir.76.3.648

Stucki AO, Stucki JD, Hall SRR, Felder M, Mermoud Y, Schmid RA, Geiser T, Guenat OT (2015) A lung-on-a-chip array with an integrated bio-inspired respiration mechanism. Lab Chip 15:1302–1310. https://doi.org/10.1039/C4LC01252F

Stucki JD, Hobi N, Galimov A, Stucki AO, Schneider-Daum N, Lehr C-M, Huwer H, Frick M, Funke-Chambour M, Geiser T, Guenat OT (2018) Medium throughput breathing human primary cell alveolus-on-chip model. Sci Rep 8:14359. https://doi.org/10.1038/s41598-018-32523-x

Tschumperlin DJ, Oswari J, Margulies SSa (2000) Deformation-induced injury of alveolar epithelial cells. Am J Resp Critical Care Med 162:357–362. https://doi.org/10.1164/ajrccm.162.2.9807003

Tzima E, Irani-Tehrani M, Kiosses WB, Dejana E, Schultz DA, Engelhardt B, Cao G, DeLisser H, Schwartz MA (2005) A mechanosensory complex that mediates the endothelial cell response to fluid shear stress. Nature 437:426–431. https://doi.org/10.1038/nature03952

Wang Y, Shyy JY-J, Chien S (2008) Fluorescence proteins, live-cell imaging, and mechanobiology: seeing is believing. Annu Rev Biomed Eng 10:1–38. https://doi.org/10.1146/annurev.bioeng.010308.161731

Wang Z, Volinsky AA, Gallant ND (2014) Crosslinking effect on polydimethylsiloxane elastic modulus measured by custom-built compression instrument. J Appl Polyr Sci. https://doi.org/10.1002/app.41050

Wong JF, Simmons CA (2019) Microfluidic assay for the on-chip electrochemical measurement of cell monolayer permeability. Lab Chip 19:1060–1070. https://doi.org/10.1039/C8LC01321G

Yang X, Li K, Zhang X, Liu C, Guo B, Wen W, Gao X (2018) Nanofiber membrane supported lung-on-a-chip microdevice for anti-cancer drug testing. Lab Chip 18:486–495. https://doi.org/10.1039/C7LC01224A

Zamprogno P, Wüthrich S, Achenbach S, Thoma G, Stucki JD, Hobi N, Schneider-Daum N, Claus-Michael L, Huwer H, Geiser T, Schmid RA, Guenat OT (2021) Second-generation lung-on-a-chip with an array of stretchable alveoli made with a biological membrane. Commun Biol. https://doi.org/10.1038/s42003-021-01695-0

Zhang M, Wang P, Luo R, Wang Y, Li Z, Guo Y, Yao Y, Li M, Tao T, Chen W, Han J, Liu H, Cui K, Zhang X, Zheng Y, Qin J (2021) Biomimetic human disease model of SARS-CoV-2-induced lung injury and immune responses on organ chip system. Adv Sci 8:2002928. https://doi.org/10.1002/advs.202002928